ENHANCING BLOOD BRAIN BARRIER PERMEABILITY OF THERAPUETIC AGENTS FOR ALZHEIMER'S DISEASE BY ADDING GLUCOSE.

by

Matthew Canipe

Submitted in partial fulfillment of the
requirements for Departmental Honors in
the Department of Chemistry
Texas Christian University
Fort Worth, Texas

May 2, 2016

ENHANCING BLOOD BRAIN BARRIER PERMEABILITY OF THERAPUETIC AGENTS FOR ALZHEIMER'S DISEASE BY ADDING GLUCOSE.

Project Approved:

Supervising Professor: Kayla N. Green, Ph.D.

Department of Chemistry & Biochemistry

Gary W. Boehm, Ph.D.

Department of Psychology

Eric E. Simanek. Ph.D.

Department of Chemistry & Biochemistry

ABSTRACT

The Green Research Group has previously synthesized molecules that are capable of combating the hallmarks of Alzheimer's disease and preventing and reversing amyloid beta aggregate formation. While preliminary studies show that these ligands are able to cross the blood brain barrier to an extent, it is important to enhance this property of the ligands. In this study, we apply a common technique to increase blood brain barrier permeability, glycosylation, to the **L2** and **L3** ligands. New synthetic pathways and reactions were created to achieve glycosylation, and the newly synthesized molecules were characterized using ^{1}H NMR, ^{13}C NMR, and mass spectrometry.

TABLE OF CONTENTS

ACKNOWLEDGEMENTS.....v

LIST OF FIGURES.....vii

LIST OF TABLES.....viii

INTRODUCTION.....9

MATERIALS AND METHODS.....14
- General Procedures 14
- Physical Methods.....14
- Synthesis of **2**.....14
- Synthesis of **3**.....16
- Synthesis of **5**.....18
- Synthesis of **6**.....22
- Synthesis of **8**.....25

RESULTS AND DISCUSSION.....30

CONCLUSIONS.....43

REFERENCES.....44

Acknowledgements

First and foremost, I would like to thank those who made attending TCU a possibility for me: my parents and TCU for awarding me with an academic scholarship. Everything I accomplished at TCU would not have been possible without this support. My accomplishments also would not have been possible without the outstanding professors I had throughout my collegiate career. They were able to challenge me in ways which developed understanding and fostered the exploration of my interests. Specifically, I would like to thank Dr. Gary Boehm for pushing me to get involved with research and Dr. Julie Fry for introducing me to Dr. Kayla Green's research.

Next, I would like to thank everyone who made my transition into the Green Research Group an easy one. Hannah Johnston, thank you for mentoring me and teaching me the ligand synthesis my first semester. You really got me interested in optimizing synthesis and derivatization of the ligands. Thank you to all of the members of the Green Research Group—past members who contributed to the synthesis and study of our ligands and the current members for making my work easier and more enjoyable.

I would now like the thank everyone who directly contributed to my project. Dr. Kayla Green, thank you for introducing me to the idea of glycosylating the ligands and allowing me to undertake this project. Sean Rodich, thank you for recommending me to use Ag_2O as a catalyst and assisting me in its use. Dr. David Minter, thank you for your assistance in determining connectivity as well as the idea to glycosylate phenol as a control. Samantha Brewer, Marianne Burnett, and Hannah Johnston, thank you for the many NMR spectra you looked at and helped me turn into figures. Thank you to my thesis committee members, Dr. Eric Simanek and Dr. Gary Boehm for your guidance throughout my project and the writing of this thesis.

Additionally, thank you to the following grants and foundations for the funding that made this research possible: TCU SERC Grant, TCU Honors Research Grant, TCU Chemistry and CSE, Welch Foundation P-1760, Moncrief Cancer Institute, TCU RCAF & Andrews Institute, The Neurobiology of Aging Collaborative at TCU.

Finally, I would like the thank Dr. Kayla Green. Thank you for welcoming me into the group and allowing me to explore my interests. Thank you for always making yourself available to assist and guide. Thank you for the countless hours you spent helping me with characterization, problem solving, writing, and editing. Throughout my time in the Green Research Group, you helped me develop into a more well-rounded student. Thank you for being a devoted and great mentor.

List of Figures

Figure Page

1. An imbalance between ROS and antioxidants in biological systems results in disease. Compound **7** has been shown to serve as an antioxidant capable of balancing the ROS/antioxidant system.....9

2. Reactive oxygen species (ROS) are produced through metal induced amyloid aggregation which leads to neuronal damage and loss associated with Alzheimer's disease.....10

3. Molecules developed by the Green Research Group can target toxic radicals and ROS generating metal-ions as well as reverse and block amyloid formation. The proposed molecules will enhance these features and target neurodegenerative hallmarks such as ROS, protein misfolding, and enhancing intracellular antioxidant defenses.....11

4. Compounds **L1** and **L2** have been shown to prevent the formation of amyloid aggregates in addition to reversing their formation.....11

5. The blood brain barrier permeability of SAM 995 was doubled upon glycosylation to produce SAM 1095.[5].....12

6. Rational design of glycosylated **L2**.....13

7. ^{1}H NMR spectrum (d_6-DMSO) of compound **2** with resonance assignments.....15

8. ^{1}H NMR spectrum (dimethylformamide-d_6) of compound **3** with resonance assignments.....17

9. ^{13}C NMR spectrum (dimethylformamide-d_6) of compound **3** with resonance assignments.....18

10. ^{1}H NMR spectrum (d_6-DMSO) of compound **5** with resonance assignments.....20

11. ^{13}C NMR spectrum (d_6-DMSO) of compound **5** with resonance assignments.....21

12. Mass spectrum of compound **5**.....22

13. ^{1}H NMR spectrum (d_6-DMSO) of compound **6** with resonance assignments.....24

14. ^{13}C NMR spectrum (d_6-DMSO) of compound **6** with resonance assignments.....25

15. ^{1}H NMR spectrum (d_6-DMSO) of compound **8** with resonance assignments.....27

16. ^{13}C NMR spectrum (d_6-DMSO) of compound **8** with resonance assignments.....28

17. Mass spectrum of compound **8**.....29

18. ^{1}H NMR of Sean Rodich's galactose product in DMSO with labeled molecular diagram.[19].....42

List of Tables

1. Comparison of the Lipinski's parameters for compound **8** and **10**.[17,18] Lipinski's rules: (low molecular weight (MW ≤ 450), relatively lipophilic (c log P, calculated logarithm of the octanol/water partition coefficient, ≤5), hydrogen-bond donor atoms (HBD ≤ 5), hydrogen-bond acceptor atoms (HBA ≤ 10).....31

2. Solvent impurities in dimethylformamide-d_6 (^{1}H NMR).....36

3. Solvent impurities in dimethylformamide-d_6 (^{13}C NMR).....37

Introduction

Alzheimer's disease is a growing problem in the world. In 2010, an estimated 4.7 million Americans were living with Alzheimer's disease, and by 2050, this number is expected to grow to 13.8 million.[1] Even more concerning, out of the leading causes of death related to diseases in the United States, Alzheimer's disease was the only disease that had an increase in the percentage of those affected since 2000.[1] All other diseases, stroke, heart disease, and cancers, have declined in the numbers dying from the disease. Part of the reason for the increase in Alzheimer's disease is due to the mechanism(s) responsible for the development of the disease are still unknown. Therefore, effective treatments have been challenging to develop.

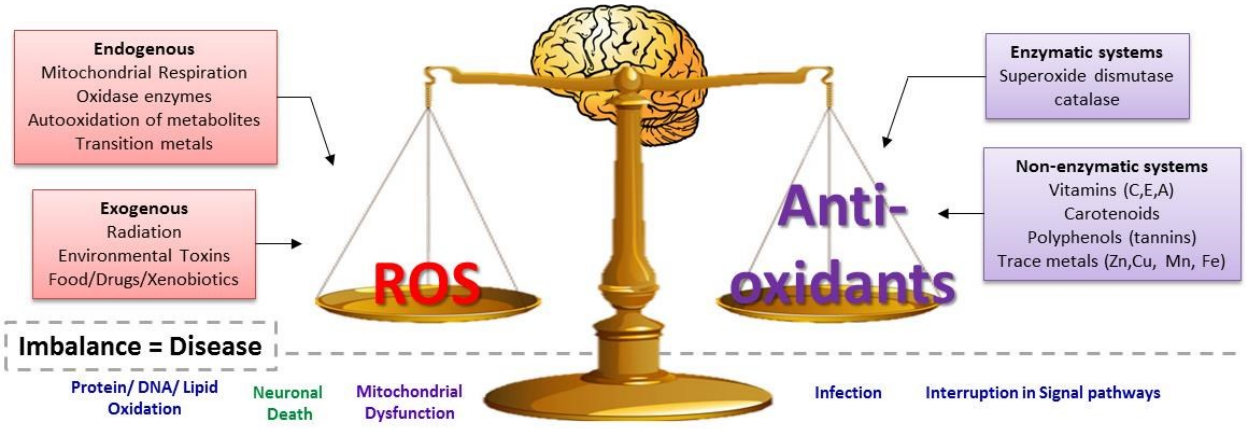

Figure 1. An imbalance between ROS and antioxidants in biological systems results in disease. Compound **7** has been shown to serve as an antioxidant capable of balancing the ROS/antioxidant system.

One hypothesis proposed for the development of the disease involves reactive oxygen species (ROS) in the form of radicals and metal ions, a decrease in antioxidant defenses, and the misfolding of the protein amyloid beta.[2] The amyloid protein is ubiquitous in nature. In healthy individuals, accumulated protein is cleared before the formation of plaques. However, in individuals affected with Alzheimer's disease, the amyloid beta protein begins to accumulate,

forming fibrils and then plaques. These aggregated proteins lead to neuronal death, which release more ROS and miscompartmentalized metal ions. While the brain, in particular, is adept at balancing ROS with antioxidants, the ROS generated through the amyloid mechanism creates an imbalance. The resulting ROS and metal ions lead to the formation of more plaques and more neuronal death (Figure 1) , forming a vicious cycle which leads to the progression of the disease (Figure 2).

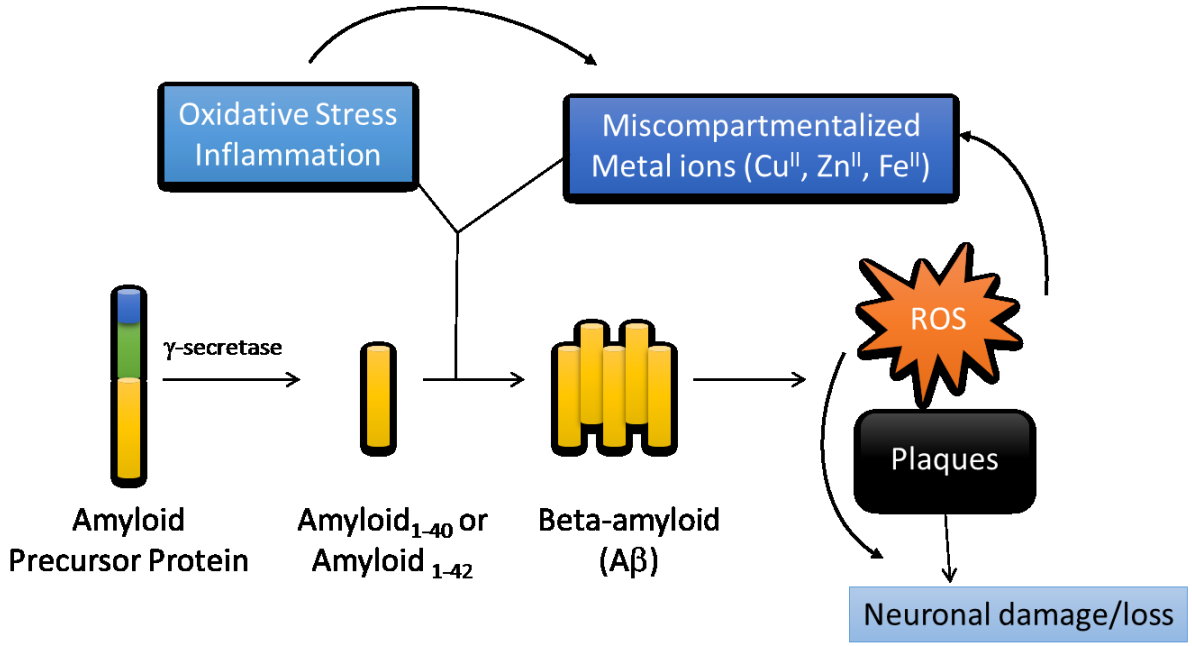

Figure 2. Reactive oxygen species (ROS) are produced through metal induced amyloid aggregation which leads to neuronal damage and loss associated with Alzheimer's disease.

The hypothesis of ROS, amyloid beta, and metal ions being causative agents in the onset and progression of Alzheimer's disease gives researchers therapeutic targets to focus on for the development of treatments for Alzheimer's disease: neutralizing ROS, sequestering metal ions, and restoring antioxidant defenses. The Green Research Group has developed an N-heterocyclic amine ligand set capable of combating each of these targets (Figure 3).[3,4]

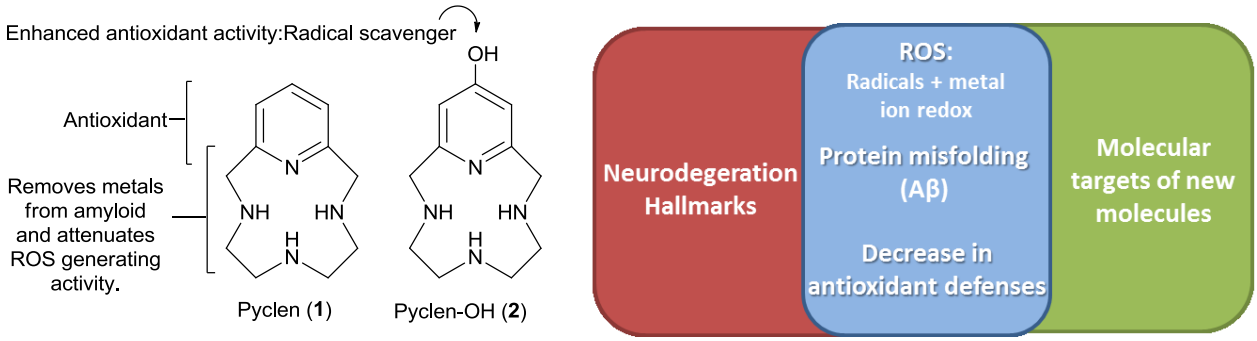

Figure 3. Molecules developed by the Green Research Group can target toxic radicals and ROS generating metal-ions as well as reverse and block amyloid formation. The proposed molecules will enhance these features and target neurodegenerative hallmarks such as ROS, protein misfolding, and enhancing intracellular antioxidant defenses.

The ligands have a strong metal binding core capable of removing metal ions from amyloid and a pyridine (**L1**) or pyridol (**L2** and **L3**) moiety that acts as an antioxidant and radical scavenger. These ligands have demonstrated the ability to both reverse and prevent the formation of the amyloid beta aggregates *in vitro* as depicted in Figure 4.[3,4]

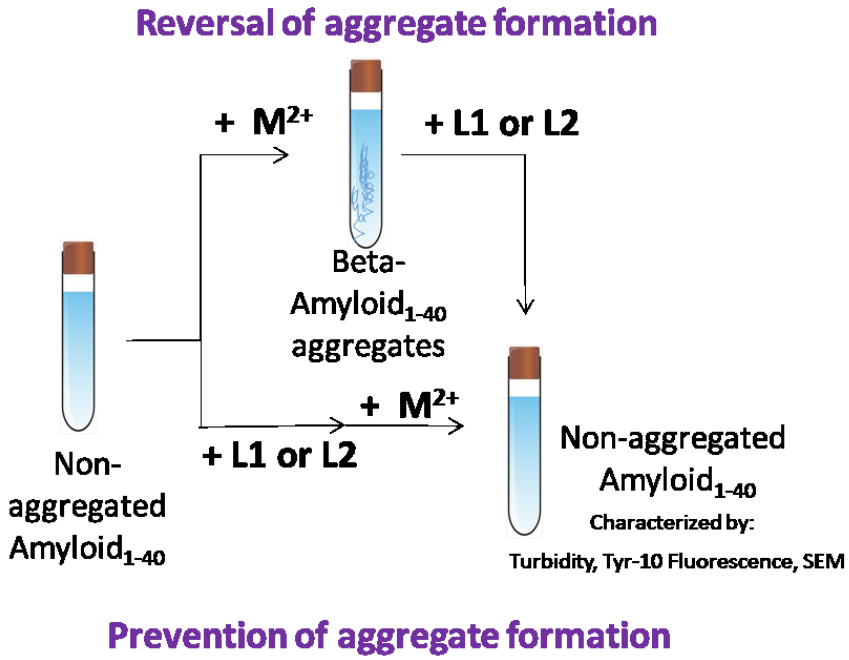

Figure 4. Compounds **L1** and **L2** have been shown to prevent the formation of amyloid aggregates in addition to reversing their formation.

While preliminary studies suggest that our ligands are successful in crossing the blood brain barrier (BBB), it is important to enhance this property of the ligands. While necessary to protect our brain from toxins and infections, the BBB can also prevent therapeutic agents from reaching the brain. Without the ability to pass this barrier, a drug designed to function in the brain is ineffective despite its reactivity in other media.

One common method of increasing the BBB permeability of a molecule is glycosylation.[5] This method is effective because the BBB contains glucose transporter 1 (GLUT1) to deliver glucose to the brain. The added glucose is able to trick GLUT1 to transport the compound across the blood brain barrier, which otherwise would not be able to enter the brain. The efficacy of this method has been reported in a multitude of studies. For example, in Egleton, R.D., *et al*., the blood brain barrier permeability of a peptide was doubled by the addition of a single glucose molecule (Figure 5).[5]

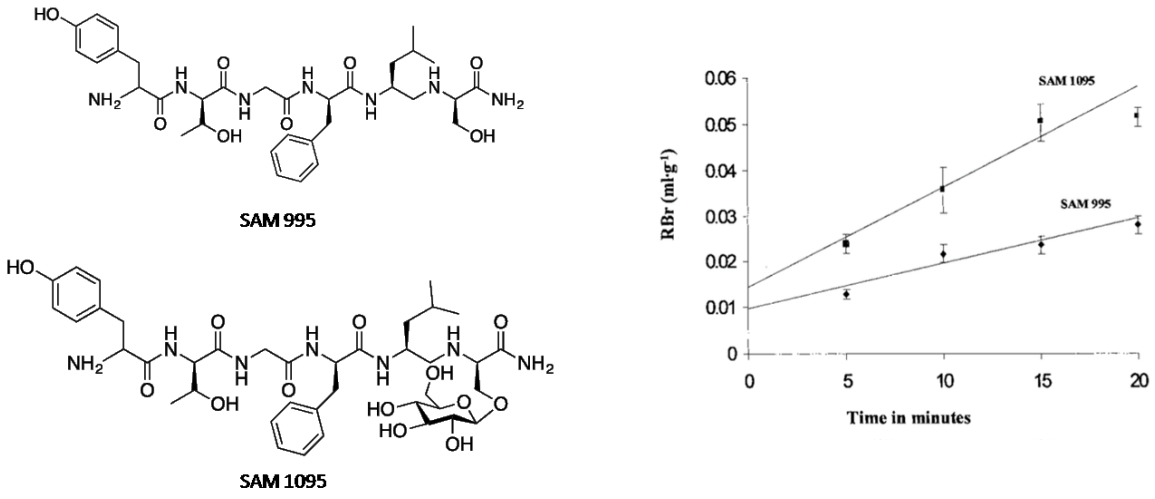

Figure 5. The blood brain barrier permeability of SAM 995 was doubled upon glycosylation to produce SAM 1095.[5]

Applying the glycosylation strategy to enhance the blood brain barrier permeability to our **L2** and **L3** ligands, we were able to design new molecules with a glucose O-linked to the pyridol

ring (Figure 6). Theoretically, these glycosylated ligands would be able to cross the BBB in quantitatively higher amounts compared to ligands **L2** and **L3**, reverse and prevent the formation of amyloid beta aggregates, and combat the progression of Alzheimer's disease.

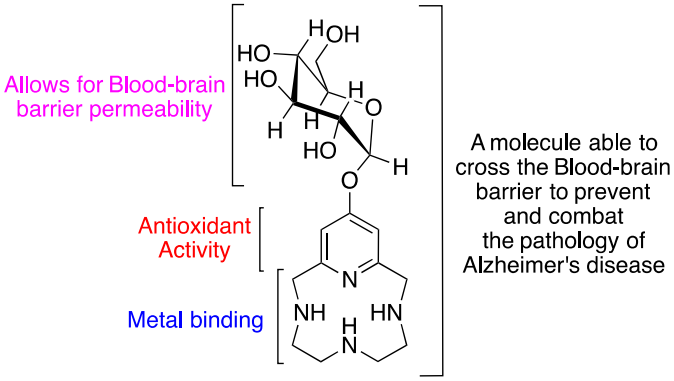

Figure 6. Rational design of glycosylated **L2**.

This thesis will focus on the methods explored to append a glucose moiety onto pyridol containing N-heterocyclic amines. The results of synthetic efforts, characterization of products, and analysis of these results will be presented herein.

Materials and Methods

General Procedures

All reagents were purchased from commercial sources and used as received unless noted otherwise. Compounds **1**, **4**, and **7** were produced using literature methods and isolated as HCl salts.[6,7]

Physical Methods

A Bruker Avance 400 MHz was utilized to obtain the NMR spectra in dimethyl sulfoxide-d_6 (DMSO) or N,N-dimethyl foramide-d_6 as specified in the sections below. HR-MS was performed using the Agilent 6224 Accurate-Mass Time-Of-Flight (TOF) MS.

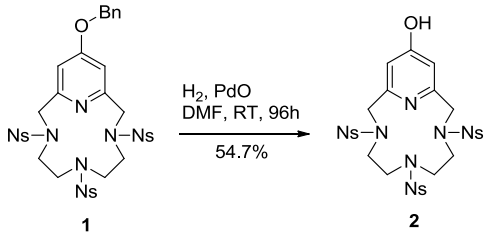

Scheme 1. Synthesis of compound **2.**

3,6,9-tris(2-nitrobenzenesulfonyl)-3,6,9,15-tetraazabicyclo[9.3.1]penta-deca-1(15),11,13-triene (Compound 2). Compound **1** was produced using methods developed by the Green Research Group.[6] Compound **1** (2.310 mmol, 2.0034 g) was added to a hydrogenation vessel along with PdO (2.451 mmol, 0.3001 g) and 40 mL of dimethylformamide. Concentrated HCl was added to this solution until the pH was measured to be 0. The vessel was purged with nitrogen, then pressurized to ~55 psi with H_2(g), and finally agitated for 96 hours. Upon completion, the

solution was syringe filtered to remove the PdO. The solvent was then evaporated under reduced pressure with several additions of toluene to form an azeotrope with the dimethylformamide. The resulting yellow solid was dissolved in chloroform. The addition of deionized H_2O resulted in the precipitation of a tan solid. This solid was isolated by vacuum filtration and was dried on a Schlenk line for several hours to yield a tan solid powder. Yield (based on compound **1**): 0.9827 g (54.7 %). ^{1}H NMR (d_6-DMSO, 400MHz) δ: 8.331 (s, 1H, residual $CHCl_3$), 7.457-6.682 (m, 14H, H_A), 4.327 (s, 4H, H_B), 3.450 (s, 2H, residual H_2O), 3.142 (s, 8H, H_C), 2.516 (s, 6H, DMSO), 2.077 (s, 3H, residual acetonitrile).

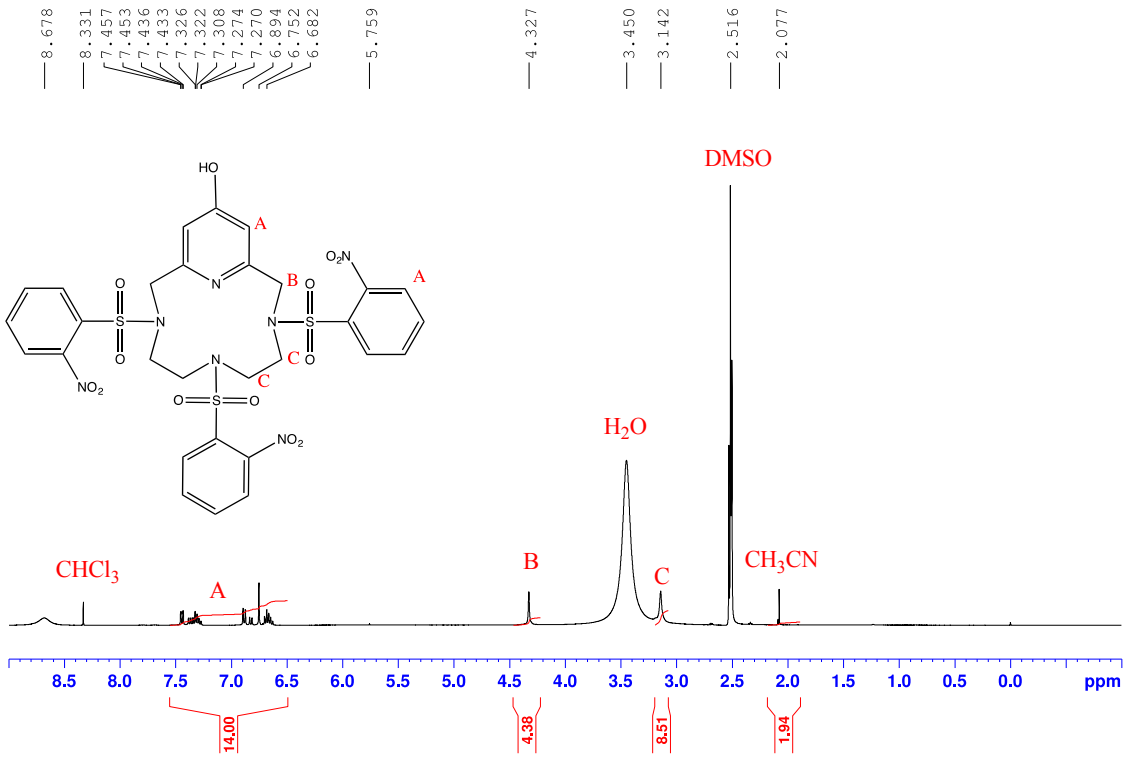

Figure 7. ^{1}H NMR spectrum (d_6-DMSO) of compound **2** with resonance assignments.

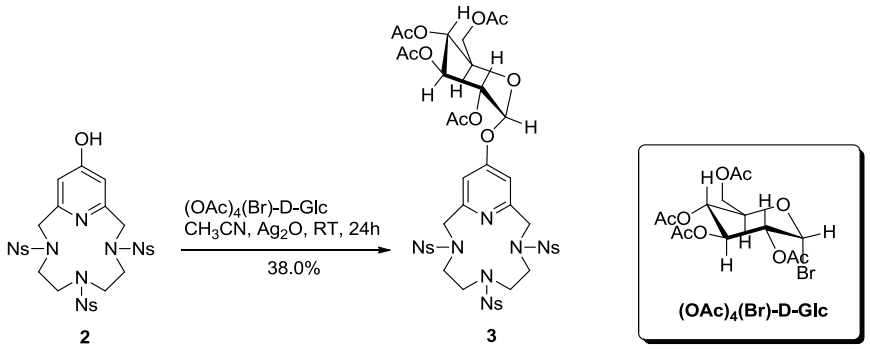

Scheme 2. Synthesis of compound **3**.

12-Aceto-D-Glucose-3,6,9-tris(2-nitrobenzenesulfonyl)-3,6,9,15-tetraazabicyclo[9.3.1]penta-deca-1(15),11,13-triene (Compound 3). Compound **2** (0.385 mmol, 299.8 mg) was added to a 125 mL round-bottom flask with 50 mL of acetonitrile. Solid Ag_2O (0.393 mmol, 161.5 mg) and Acetobromo-D-Glucose (1.071 mmol, 248.2 mg) were added to the flask, which was then covered in foil and sealed with a septum. After 24 hours, the solution was filtered through Celite to remove the Ag_2O. The solvent was then evaporated under reduced pressure. A reddish-brown powder formed and was dried on a Schlenk line. Yield (based on compound **2**): 162.3 mg (38.0%). ^{1}H NMR (dimethylformamide-d6, 400MHz) δ: 8.045 (s, dimethylformamide-d6), 7.608-6.697 (m, 14H, H_A and H_{Ns}), 7.591-7.367 (m, residual toluene), 5.560-5.077 (m, 4H, H_E, H_F, H_G, H_I), 4.530 (m, 2H, H_J), 4.322 (s, 4H, H_B), 4.252 (m, 1H, H_H), 3.602 (s, residual methanol), 3.499 (q, residual ether), 3.296-3.188 (m, 8H, H_C and H_D), 2.930 (s, dimethylformamide-d6), 2.856 (s, dimethylformamide-d6), 2.382 (s, residual toluene), 2.122-2.021 (m, 12H, H_K), 1.867 (s, residual acetonitrile), 1.292 (s, residual hexanes), 1.128 (t, residual ether), 0.864 (s, residual hexanes). ^{13}C NMR (dimethylformamide-d6, 100MHz) δ: 170.23-169.34 (4C, C_M), 158.24 (C_A), 155.70 (C_C), 147.57-146.80 (3C, C_{Ns}-NO_2), 139.41 (residual toluene), 134.12 (residual toluene), 129.76 (residual toluene), 120.57-115.90 (C_{Ns}), 113.63 (residual acetonitrile), 110.63 (C_B), 96.38 (C_G),

74.19-65.83 ($C_{H, I, J, K, L}$), 60.85 (C_D), 54.81 (residual dichloromethane), 47.40 (C_E), 45.22 (residual methanol), 38.91 (C_F), 22.22 (residual toluene), 20.05-19.91 (C_N).

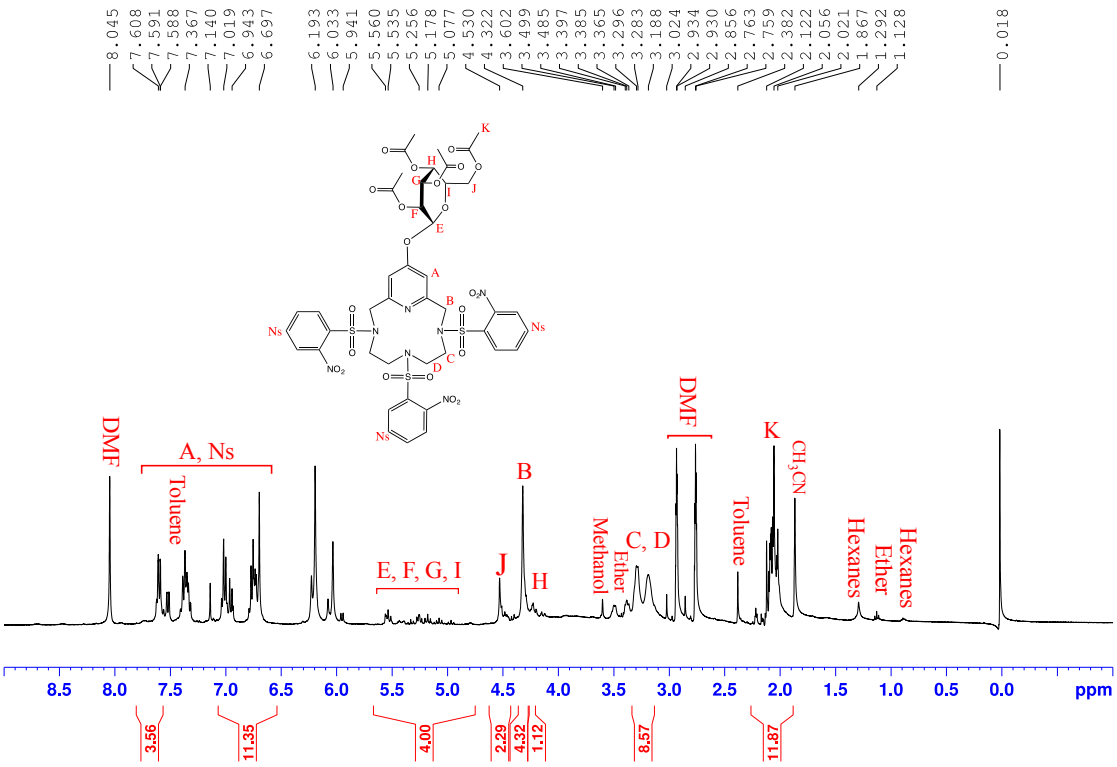

Figure 8. ^{1}H NMR spectrum (dimethylformamide-d_6) of compound **3** with resonance assignments.

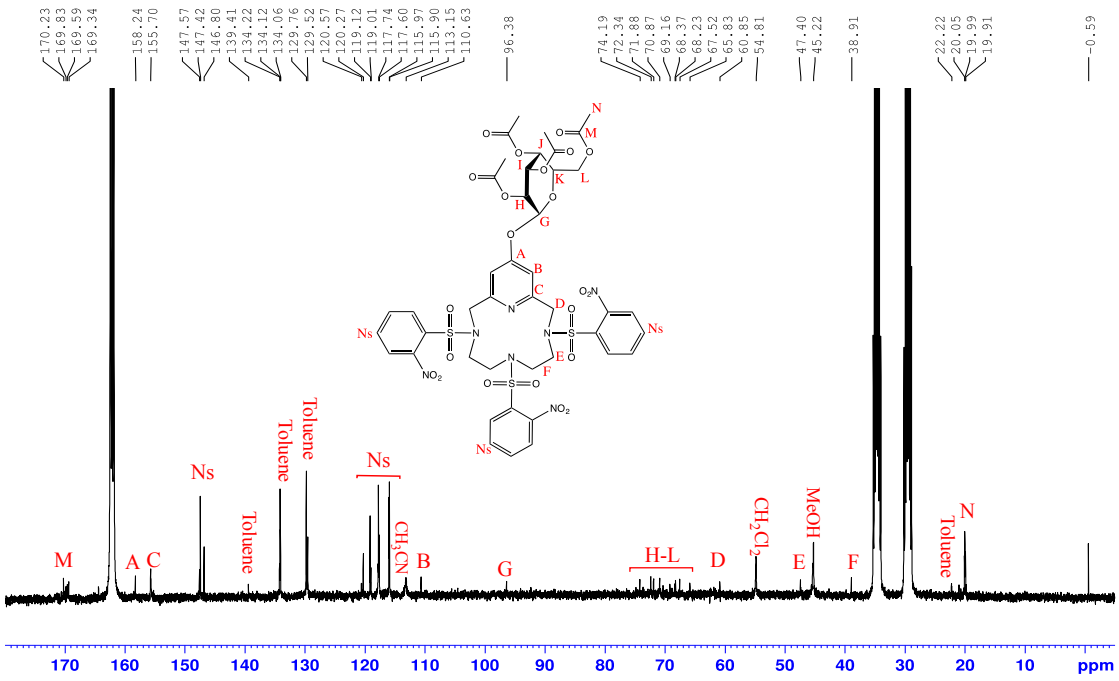

Figure 9. ^{13}C NMR spectrum (dimethylformamide-d_6) of compound **3** with resonance assignments.

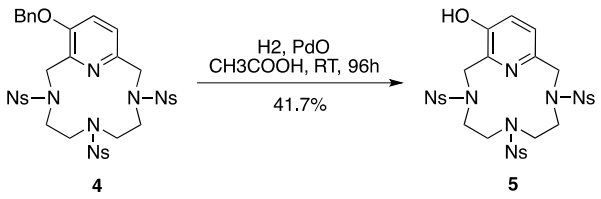

Scheme 3. Synthetic pathway used to produce compound **5**.

3,6,9-tris(2-nitrobenzenesulfonyl)-3,6,9,15-tetra-azabicyclo[9.3.1]penta-deca-1(15),11,13-triene (Compound 5). Compound **4** was produced using methods developed by the Green Research Group.[7] Solid compound **4** (2.314 mmol, 2.0072 g) was added to a hydrogenation vessel along with PdO (2.463 mmol, 0.3015 g) and 100 mL of Acetic Acid. The vessel was purged with nitrogen, pressurized to ~55 psi with H_2(g), and then agitated for 96 hours. Upon completion, the solution

was syringe filtered to remove the PdO and the solvent was evaporated under reduced pressure. This resulted in a brown oil which yielded a dark brown solid after several hours on a Schlenk line. Column chromatography (5% methanol in dichloromethane, silica) was used to separate three products. Compound **5** was isolated as the first fraction as a tan powdery solid after removal of solvent. Yield (Based on compound **4**): 0.7506 g (41.7%). ^{1}H NMR (d_6-DMSO, 400MHz) δ: 7.571-7.421 (m, residual toluene), 7.378-6.604 (m, 14H, $H_{A, B, Ns}$), 5.224 (s, residual dichloromethane), 4.513 and 4.360 (s, 4H, H_C), 3.347 (s, residual H_2O), 3.190-2.974 (m, 8H, $H_{D, E}$), 2.500 (s, DMSO), 2.3001 (s, residual toluene), 2.006 (m, residual acetic acid), 1.227 (s, residual hexanes), 0.846 (t, residual hexanes). ^{13}C NMR (d_6-DMSO, 100MHz) δ: 152.56 (C_A), 147.46-116.02 ($C_{B, C, D, E, Ns}$ and residual toluene), 53.77 (C_F), 49.19 (C_G), 46.53 (C_H). (ESI-TOF) m/z: $[M + H]^+$ Calcd for $C_{29}H_{28}N_7O_{13}S_3$ 778.0907; Found 778.2297.

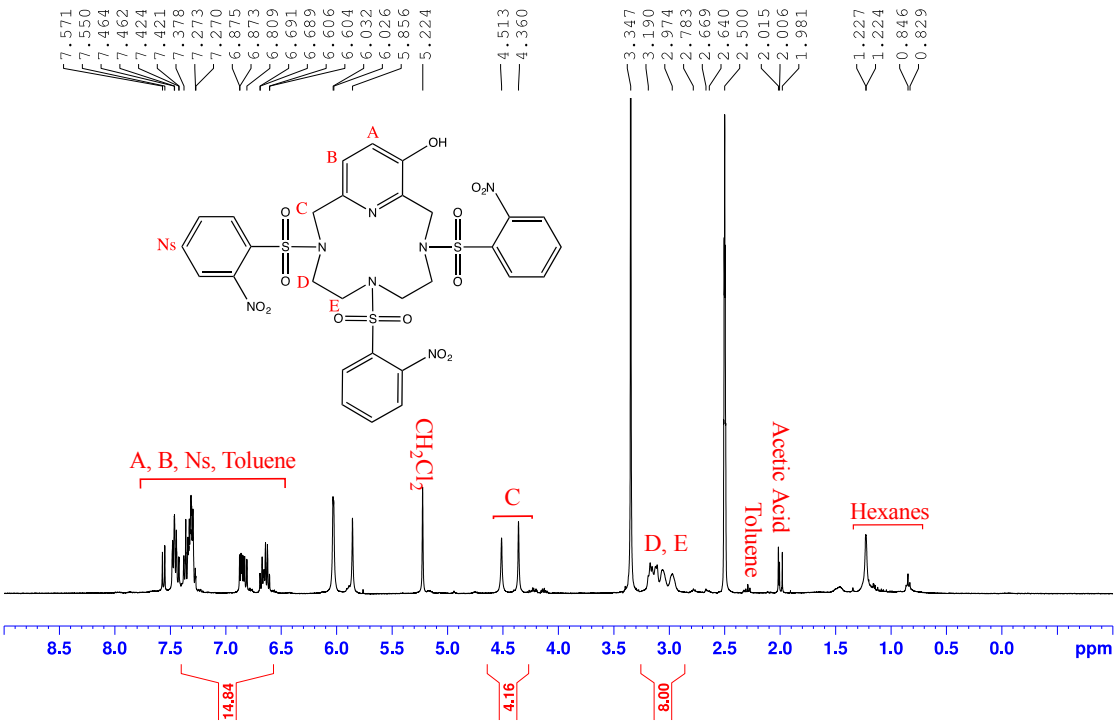

Figure 10. ^{1}H NMR spectrum (d_6-DMSO) of compound **5** with resonance assignments.

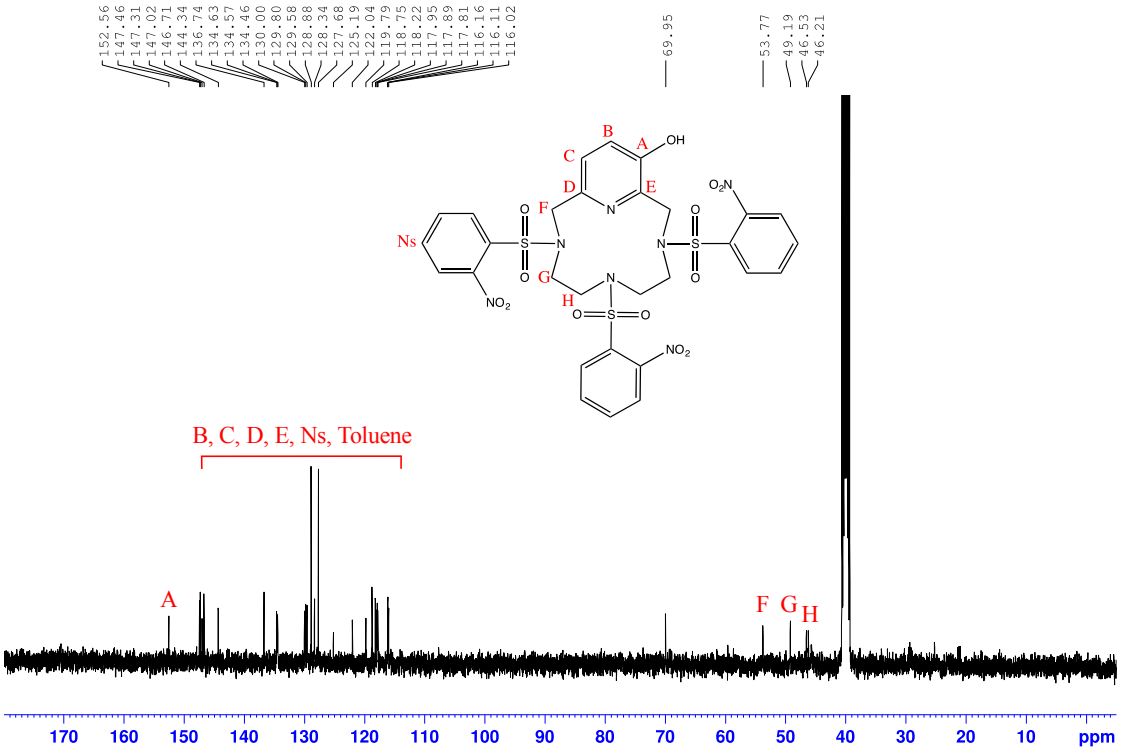

Figure 11. ^{13}C NMR spectrum (d_6-DMSO) of compound **5** with resonance assignments.

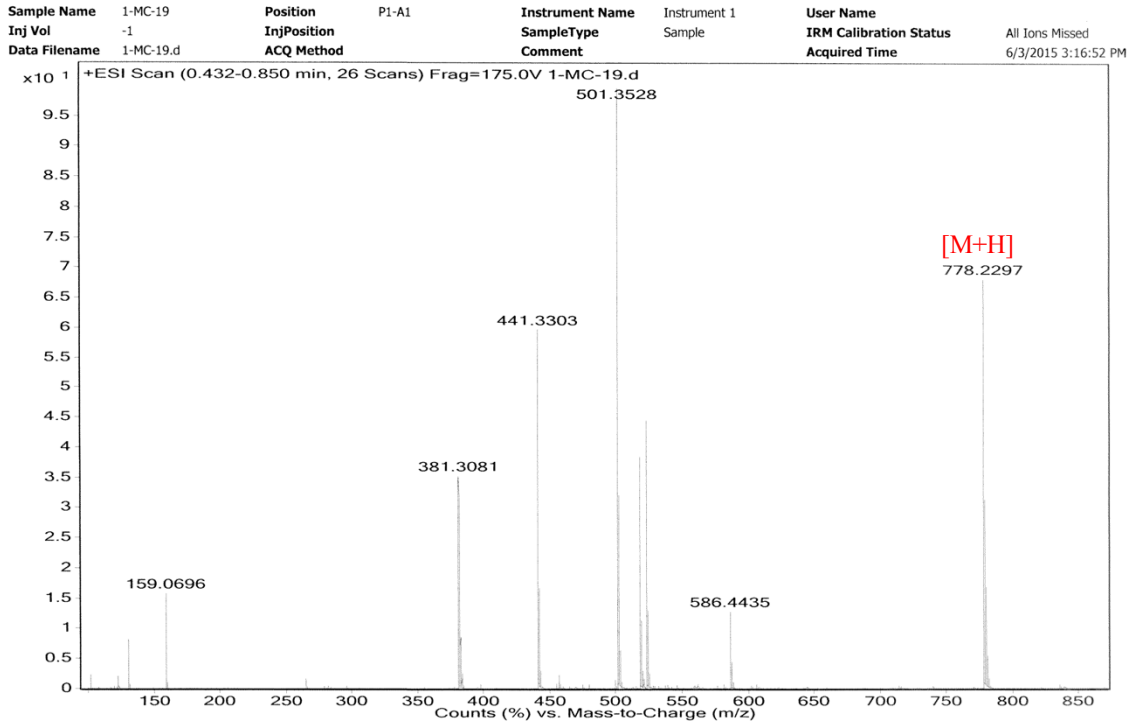

Figure 12. Mass spectrum of compound **5**.

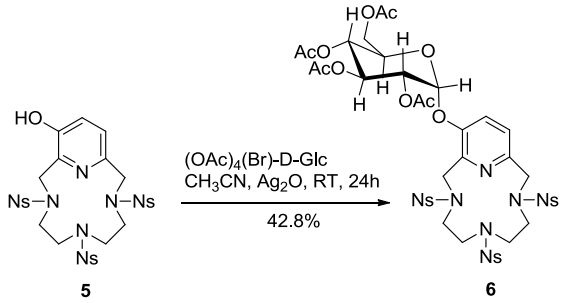

Scheme 4. Synthetic pathway used to produce compound **6**.

12-Aceto-D-Glucose -3,6,9-tris(2-nitrobenzenesulfonyl)-3,6,9,15-tetra-azabicyclo[9.3.1]penta-deca-1(15),11,13-triene (Compound 6). Compound **5** (0.386 mmol, 300.2 mg) was added to a 125 mL round-bottom flask with 50 mL of acetonitrile. Ag_2O (0.421 mmol, 173.2 mg) and Acetobromo-D-Glucose

(0.789 mmol, 182.9 mg) were added to the flask, which was then covered in foil and sealed with a septum. After 24 hours, the solution was filtered through Celite to remove the Ag_2O. The solvent was then evaporated under reduced pressure resulting in a tacky oil. The addition of ether yielded a tan, powdery precipitate. This solid isolated and was then dried on a Schlenk line for several hours. Yield (based on compound **5**): 358.0 mg (42.8%). ^{1}H NMR (d_6-DMSO, 400MHz) δ: 7.571-7.421 (m, residual toluene), 7.378-6.604 (m, 14H, $H_{A, B, Ns}$), 5.382 (t, 1H, H_F), 5.194-4.693 (m, 3H, $H_{G, H, J}$), 4.513 and 4.360 (s, 4H, H_C), 4.266-3.945 (m, 3H, $H_{I, K}$), 3.353 (q, residual ether), 3.172-2.972 (m, 8H, $H_{D, E}$), 2.344 (s, residual toluene), 2.075 (m, 12H, H_L), 1.227 (s, residual hexanes), 1.090 (t, residual ether), 0.846 (t, residual hexanes). ^{13}C NMR (d_6-DMSO, 100MHz) δ: 170.49 (residual acetic acid), 170.27-169.72 (4C, C_O), 152.57 (C_A), 147.46-116.03 ($C_{A, B, C, D, E, Ns}$ and residual toluene), 91.41 (C_I), 72.78-65.40 ($C_{J, K, L, M, N}$), 61.93 (residual ether), 53.78 (C_F), 46.20 (C_G), 45.71 (C_H), 21.30-20.85 (C_P, residual acetic acid, residual toluene), 15.65 (residual ether).

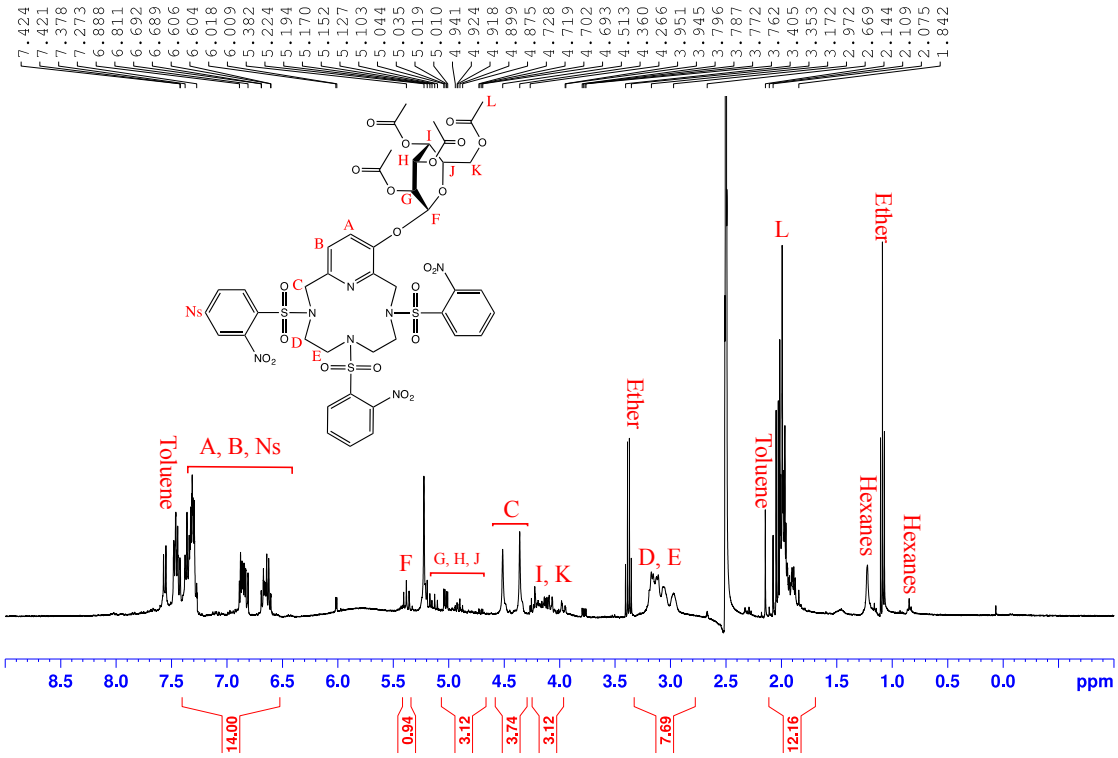

Figure 13. ^{1}H NMR spectrum (d_6-DMSO) of compound **6** with resonance assignments.

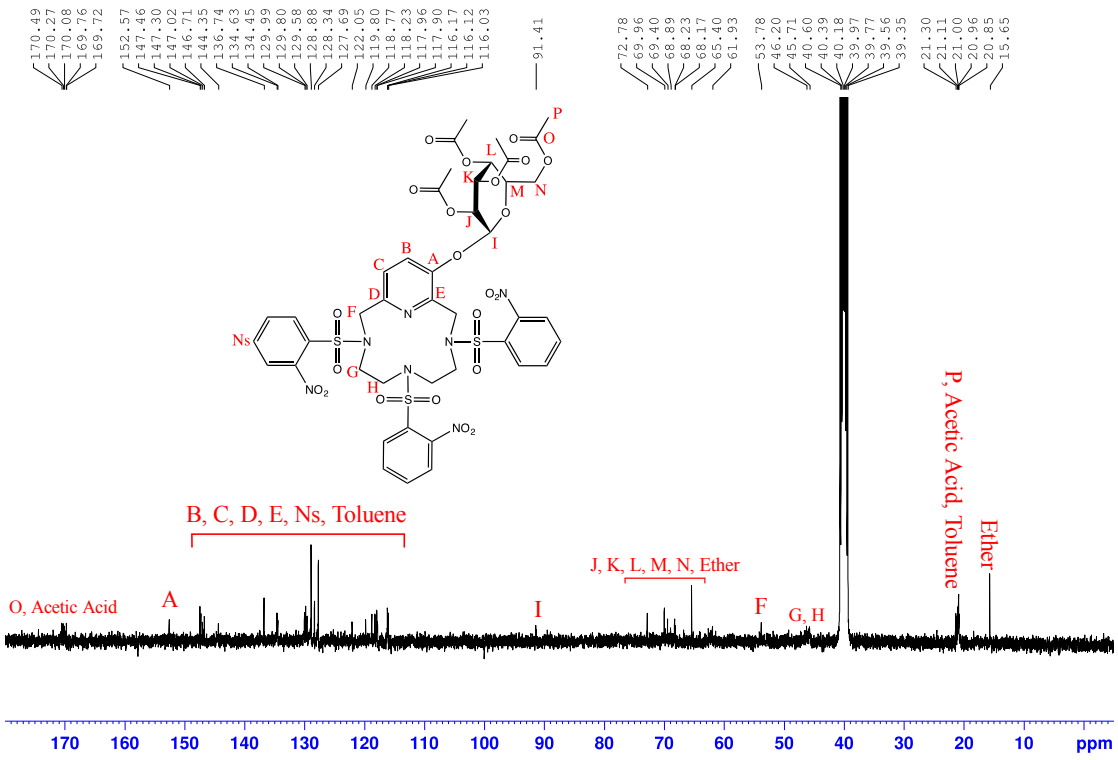

Figure 14. ^{13}C NMR spectrum (d_6-DMSO) of compound **6** with resonance assignments.

Synthesis of Compound **8**:

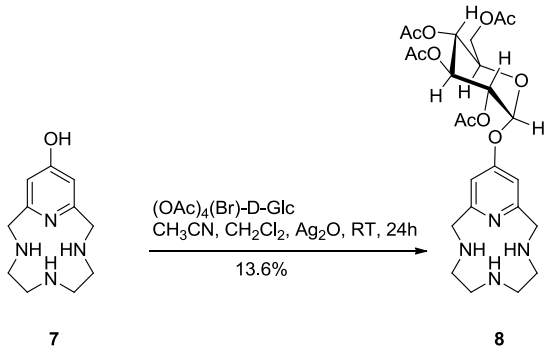

Scheme 5. Synthetic pathway used to produce compound **8**.

12-Aceto-D-Glucose-3,6,9,15-tetraazabicyclo[9.3.1]penta-deca-1(15),11,13-trien-13-ol (Compound 8).

Compound **7** was produced using methods developed by the Green Research Group.[6] Compound **7** (0.480 mmol, 202.3 mg) was added to a 125 mL round-bottom flask with 20 mL of acetonitrile and 20 mL of dichloromethane. Solid Ag_2O (0.549 mmol, 225.8 mg) and Acetobromo-D-Glucose (0.618 mmol, 143.3 mg) were added to the flask, which was then covered in foil and sealed with a septum. After 24 hours, the solution was filtered through Celite to remove the Ag_2O. The filter was then washed with ethyl acetate. The solvent was then evaporated under reduced pressure and the resulting solid was dried on a Schlenk line for several hours. The flask was then scraped, washed with ether, and the solid was isolated via vacuum filtration. Yield (based on compound 7): 36.2 mg (13.6%). ^{1}H NMR (d_6-DMSO, 400MHz) δ: 6.397 (s, 2H, H_A), 5.763 (s, residual dichloromethane), 5.406 (m, 1H, H_E), 5.138-5.018 (m, 3H, $H_{F, G, I}$), 4.439-4.086 (m, 3H, $H_{H, J}$), 3.791 (s, 4H, H_B), 3.375 (b, residual H_2O), 2.834-2.688 (m, 8H, $H_{C, D}$), 2.020 (m, 12H, H_K and residual ethyl acetate), 1.236 (s, residual hexanes), 1.172 (t, residual ethyl acetate), 0.855 (t, residual hexanes). ^{13}C NMR (DMSO, 100MHz) δ: 170.59 (residual ethyl acetate), 170.46-169.59 (C_M), 163.57 (C_A), 160.39 (C_C), 108.35 (C_G (one isomer)), 107.17 and 102.70 (C_B), 96.05 (C_G (other isomer)), 73.95-67.39 ($C_{K, I, H, J, L}$), 65.67 (residual ether), 60.88 (residual ethyl acetate), 52.14 (residual dichloromethane), 51.57 (C_D), 46.48-46.17 ($C_{E, F}$), 21.01-20.74 (C_N and residual ethyl acetate). (ESI-TOF) m/z: $[M + H]^+$ Calcd for $C_{25}H_{37}N_4O_{10}$ 553.2510; Found 553.2822.

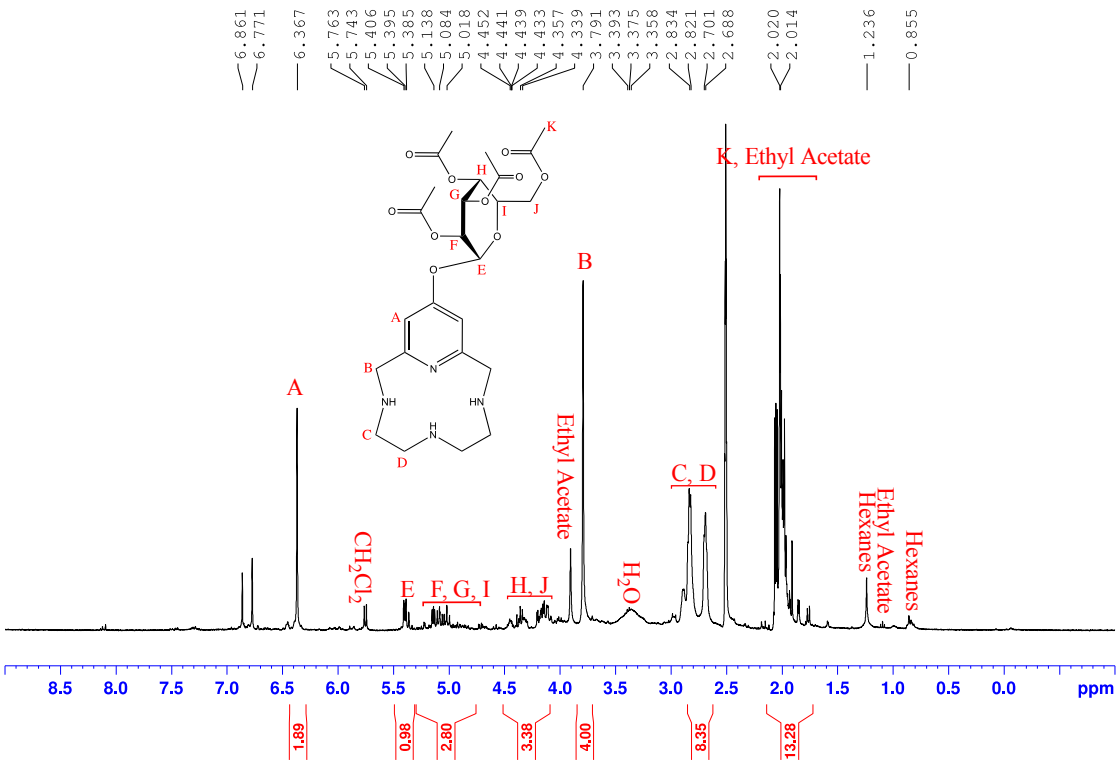

Figure 15. ^{1}H NMR spectrum (d_6-DMSO) of compound **8** with resonance assignments.

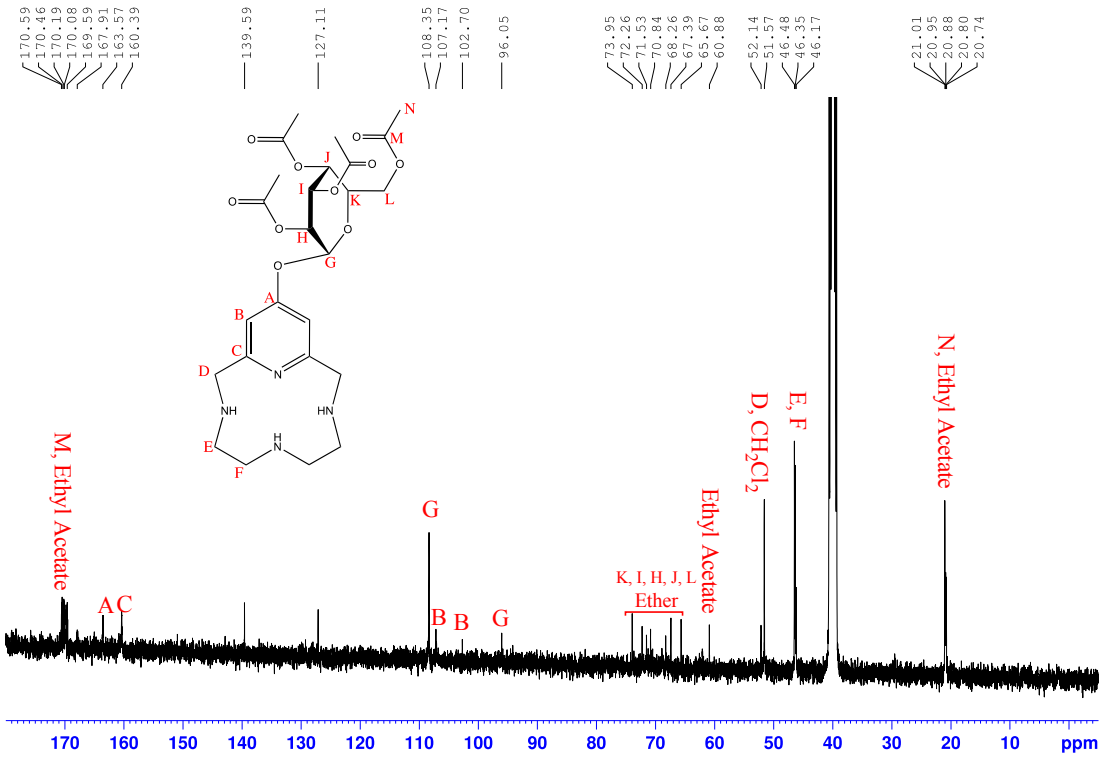

Figure 16. ^{13}C NMR spectrum (d_6-DMSO) of compound **8** with resonance assignments.

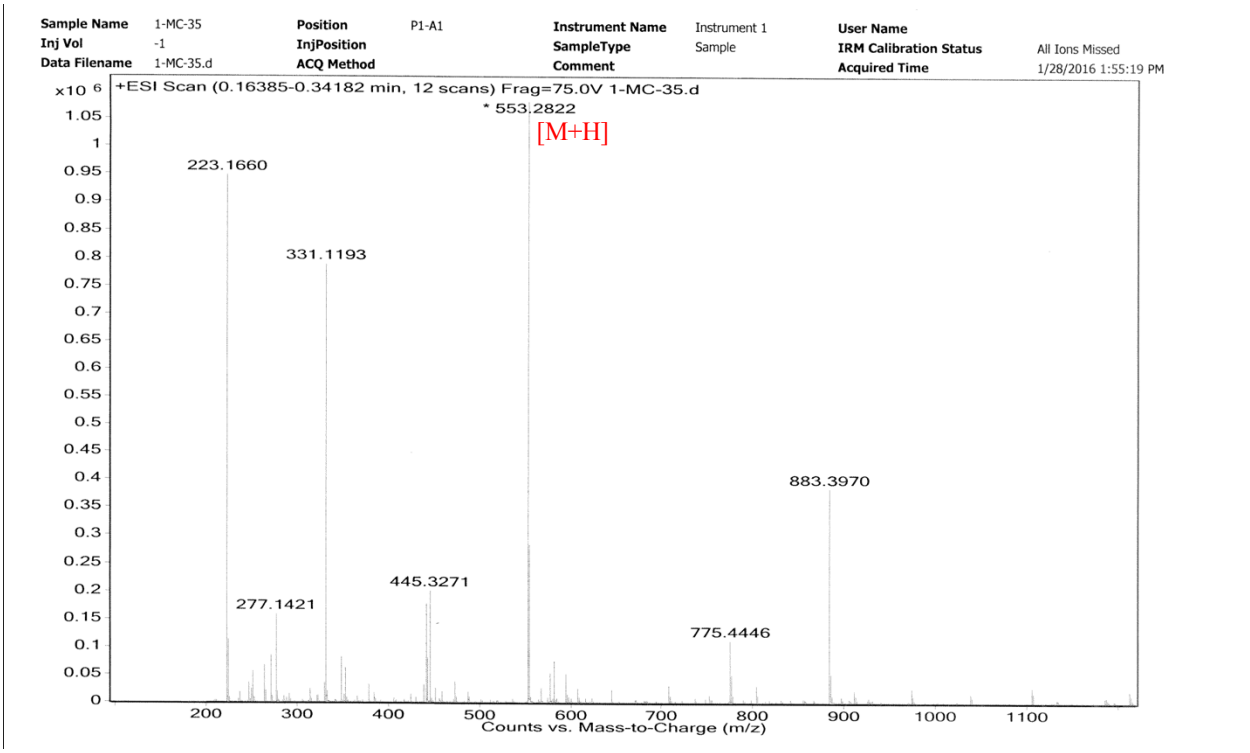

Figure 17. Mass spectrum of compound **8**.

Results and Discussion

Synthetic Design: The ability of therapeutic agents to cross the defense mechanism of the brain, the blood-brain barrier (BBB), is critical in the treatment of neurological diseases such as Alzheimer's disease. If the drug is unable to cross this barrier, it would be unable to neutralize the reactive oxygen species and break apart the amyloid plaques that are known to progress Alzheimer's disease. The Green Research Group has already synthesized molecules that are capable of combating the molecular features that progress Alzheimer's, but the ability of these molecules to cross the blood-brain barrier is still not fully quantified or understood. For my project, I will address this question by engineering our molecules to specifically cross the blood-brain barrier. To do this, I have attached a glucose molecule to our **L2** and **L3** molecules. Attaching glucose increases the ability for molecules to cross the blood-brain barrier because our brains require and take up large amounts of glucose.[8]

The target compounds described herein contain the glucose moiety tethered to the potent antioxidant molecule **L2**.[6,9] The addition of a carbohydrate moiety, i.e. glucose, has been a successful method of enhancing BBB penetrability due to the high level of glucose transporters related to the brain.[8,10-12] A growing body of knowledge links diabetes, AD, and oxidative stress, thus supporting this approach.[13,12,14,15] The series of compounds produced through my project are expected to retain the antioxidant and amyloid disaggregating core of **L2**[6,16] but have the addition of glucose to enhance BBB uptake. The linkage modifications provide logP values and molecular weights within the constraints predicted for BBB uptake (see Table 1).[17,18] Compounds described in this thesis will be the first examples of glucose appended N-heterocyclic amines and will find utility in other fields (imaging/diabetes) as well.

Table 1. Comparison of the Lipinski's parameters for compound **8** and **10**.[17,18] Lipinski's rules: (low molecular weight (MW ≤ 450), relatively lipophilic (c log P, calculated logarithm of the octanol/water partition coefficient, ≤5), hydrogen-bond donor atoms (HBD ≤ 5), hydrogen-bond acceptor atoms (HBA ≤ 10).

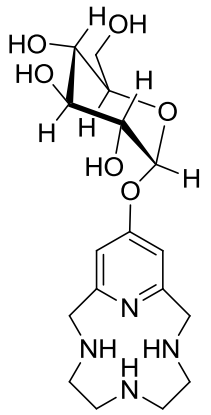

Molecular Weight: 384.4274
tPSA: 172.11
CLogP: -0.0801525
HBD< 5
HBA <10

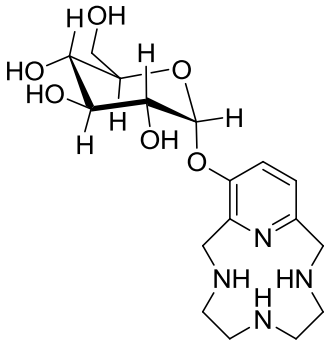

Molecular Weight: 384.4274
tPSA: 147.83
CLogP: -2.73795
HBD< 5
HBA <10

Substitution of the hydroxyl group on pyridol containing molecules is challenging and has proven to be a substantial hurdle for the Green Research Group in recent years. However, team member, Sean Rodich, was following a literature procedure to accomplish the substitution of *p*-hydroxybenzaldehyde with a galactose derivative using a silver catalyst (Scheme 6).[19] Sean's experience with this reaction encouraged me to proceed with a similar reaction for the attachment of glucose onto the pyridol ring of **L2** and **L3** using similar conditions.

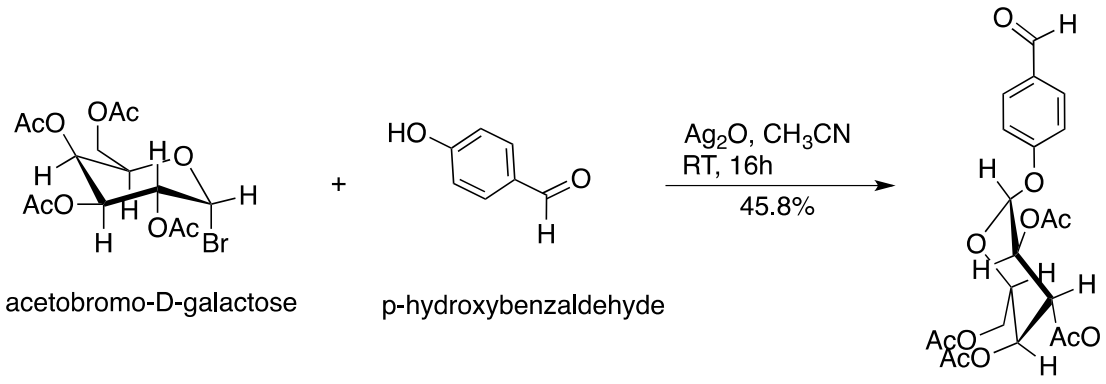

Scheme 6. The reaction of acetobromo-α-D-galactose and *p*-hydroxybenzaldehyde proceeds smoothly with Ag_2O in acetonitrile.[19]

Reaction Considerations: The addition of a glucose appendage to the Green Research Group's **L2** and **L3** ligands, based on literature precedent,[20] should proceed smoothly to produce the ether type molecules shown in Table 1. The reactive phenols are available for reactivity within compounds **2** and **7** for derivatives of **L2** and compounds **5** and **9** for derivatives of **L3**. As compounds **7** and **9** are more challenging to produce synthetically, due to being later products in the overall reaction scheme used to produce **L2** and **L3**, compounds **2** and **5** were glycosylated

first as a mean of assessing the potential for the reaction to be successful in heterocyclic systems.

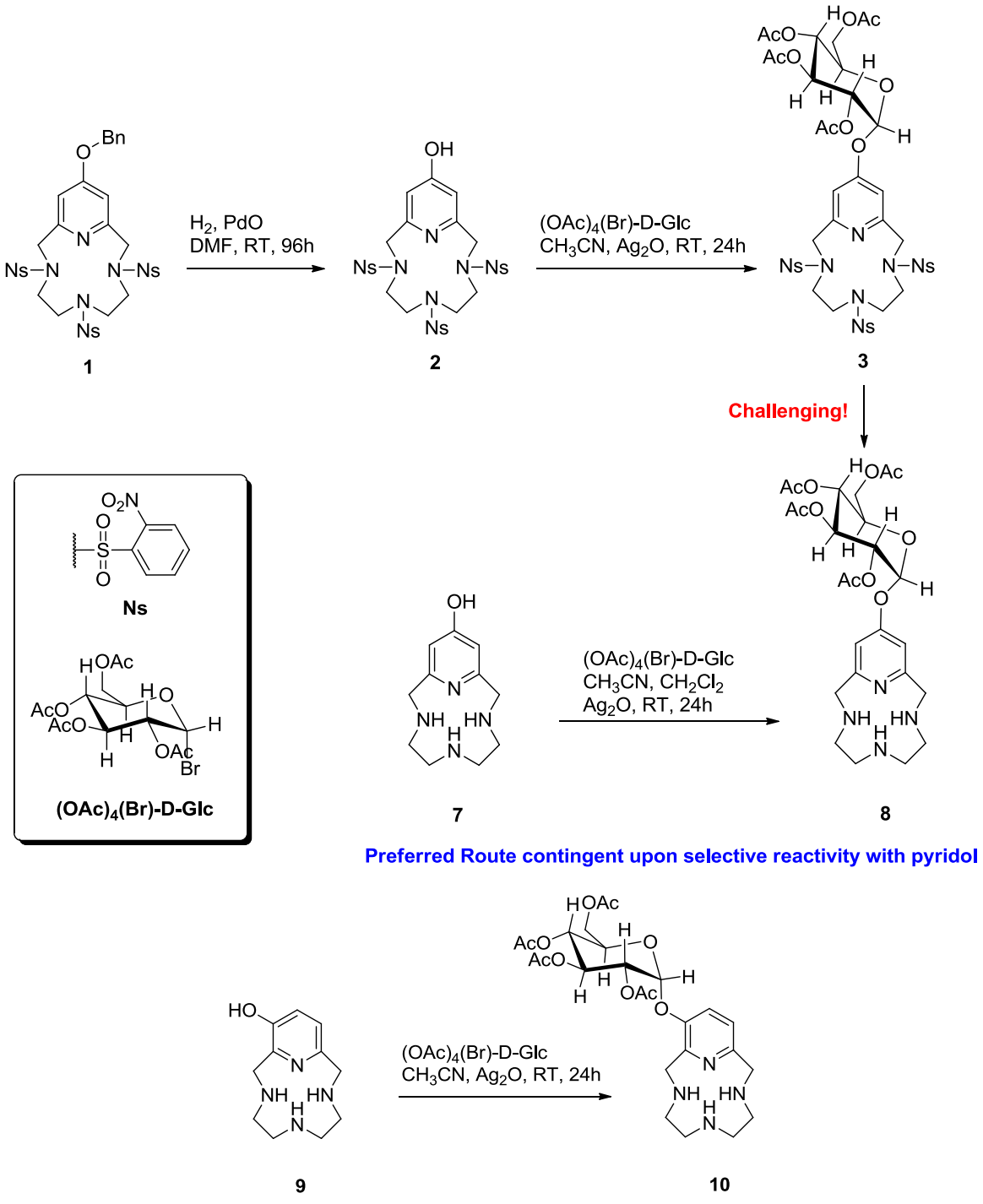

Scheme 7. Possible routes of synthesis.

Additionally, the reactivity of the phenol group vs. the reactivity of the free amine nitrogen atoms in compounds **7** and **9** was an additional concern. Therefore, despite the challenging deprotection to obtain compounds **8** from **3** (Scheme 7), pathway 1a (Scheme 8) and 1b (Scheme 9) were used to help validate the potential of the reaction to couple glucose onto the pyridol ring of the macrocyclic ligand backbones of **L2** and **L3**, optimize reaction conditions, and assist in characterization of the glycosylated compounds.

Path 1a:

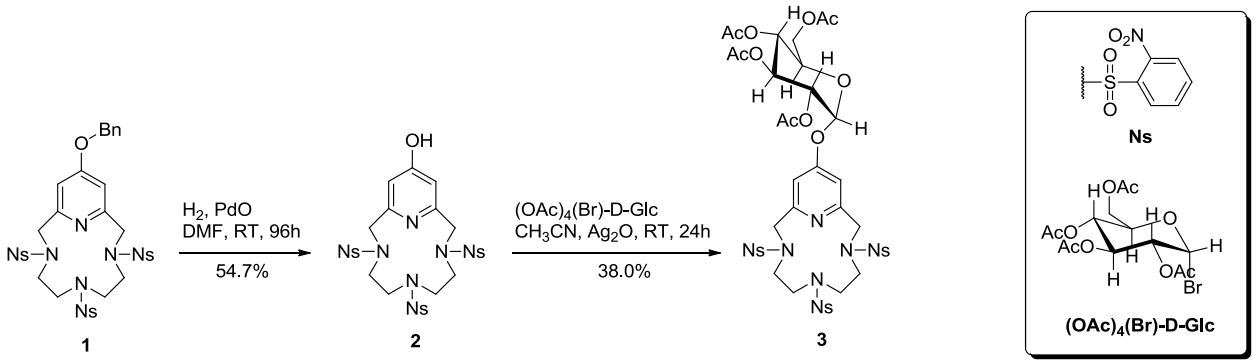

Scheme 8. Synthetic pathway used to produce compound **3**.

The first step to obtaining a glycosylated product required a free phenol, which would serve as the glycosyl acceptor. Starting synthesis with this nosylate (Ns) protected compound allowed us to test the reactivity of the phenol of **L2** in glycosylation without risking the amine nitrogens acting as a competing glycosyl group acceptor. Compound **1** is an intermediate used by the Green Research Group to produce 12-membered N-heterocyclic amines akin to compound **7**. Typically, the Nosylate protecting groups are first removed, followed by removal of the benzyl

protecting group by hydrogenation of the reactant in H_2O with PdO to yield **L2**. However, because this synthesis required deprotection of the benzyl group before removal of the nosylate groups, a novel deprotection reaction was required.

Solubility was a major challenge in the benzyl deprotection of Compound **1**. Interestingly, compound **1** was not soluble in water, resulting in unsuccessful deprotection under the Green Research Group's typical deprotection conditions (PdO, H_2, in H_2O). Hydrogenation in chloroform and acetic acid also failed as reaction solvents due to solubility issues with compound **1**. Dimethylformamide proved to provide sufficient solubility of compound **1** and H_2(g) solubility to facilitate the removal of the benzyl protecting group, thereby yielding compound **2**. The characterization of this compound (**2**) was also challenging due to solubility. The Green Research Group has noted a similar lack-of-solubility with other free –OH based heterocycles. Compound **2** was not sufficiently soluble in the majority of deuterated solvents readily available to obtain a ^{13}C NMR. Additionally, this macrocycle did not provide measurable species via mass spectrometry methods, which the Green Research Group has noted for other heterocyclic molecules of interest. Fortunately, compound **2** was obtained as a sufficiently pure sample providing enough miscibility in dimethylsulfoxide-d_6 to measure a ^{1}H NMR, thus allowing sufficient characterization for this starting material. The ^{1}H NMR spectrum showed resonances and integrations that were consistent with the connectivity shown in Figure 7, most notability the absence of resonances associated with the benzyl protecting group.

With the free phenol of compound **2** achieved, synthesis proceeded to the glycosylation step using the reaction conditions shown in Scheme 2. Again, solubility was a major challenge in this reaction. Out of the two commonly used glycosylation solvents[20], acetonitrile and dichloromethane, compound **2** was only slightly soluble in acetonitrile. Therefore, not all of the

starting material (**2**) dissolved in the reaction mixture. For this reaction, compound **2** was combined with Ag_2O and acetobromo-D-Glucose, covered with foil, and reacted for 24 h. Following the reaction work-up, the product (**3**) was isolated as a yellow solid. This low solubility of compound **2** likely contributed to the low yield (38%) of compound **3** as these reactions are typically moderate to high yielding[20]. We are currently looking into more unconventional glycosylation solvents, such as dioxane and dimethylformamide, to optimize this reaction. Finally, obtaining compound **3** as a solid was initially difficult. Removal of the reaction solvent left behind a dark oil, which is not entirely surprising as many macrocycles are known to be isolated as oils for a number of reasons, but nevertheless a complication in work-up. Several methods used by the Green Research group to isolate solid macrocycles, including the addition of toluene, hexanes, or ether/methanol, were applied to isolate a solid **3** from this oil. None of these additions were successful. Solid compound **3** was finally obtained through extensive drying on a Schlenk line and then the lyophilizer. While solvent impurities were remaining in this product, we proceeded with characterization as this reaction served as a control and proof of principle for success of this reaction.

NMR spectra were only measurable using dimethylformamide-d_6, for which data on common solvent impurities has not yet been published, to the best of our knowledge. To correct for solvents remaining in compound **3**, we added several of our commonly used solvents noted above to dimethylformamide-d_6 and obtained ^1H and ^{13}C NMR spectra. The results are listed in Table 2 & 3

Table 2. Solvent impurities in dimethylformamide-d_6 (^1H NMR).

	proton	mult	resonance
solvent residual peak	CH	s	8.043

	CH_3	s	2.934
	CH_3	s	2.764
acetonitrile	CH_3	s	2.164
chloroform	CH	s	8.386
dichloromethane	CH_2	s	5.832
diethyl ether	CH_3	t, 7	1.131
	CH_2	q, 7	3.425
methanol	CH_3	s	3.537
toluene	CH_3	s	2.337
	CH	m	7.2-7.3

Table 3. Solvent impurities in dimethylformamide-d_6 (^{13}C NMR).

	carbon	resonance
solvent residual peak	CH	162.12
	CH_3	34.63
	CH_3	29.50
acetonitrile	CN	117.64
	CH_3	0.38
chloroform	CH	79.19
dichloromethane	CH_2	54.82
diethyl ether	CH_3	14.92
	CH_2	65.32
methanol	CH_3	48.49
toluene	CH_3	20.69
	C	137.74
	CH	129.02
	CH	128.28
	CH	125.38

After eliminating these solvent impurities from the spectrum, the resonances expected for the connectivity of compound **3**, as shown in figure 8, were readily identified. Aside from residual

solvents, no other impurities proved to be present, thus encouraging us to continue with this type of reaction using Ag_2O as a catalyst for glycosylation reactions with **L2** and **L3.**

The synthetic path used to install glucose onto the –OH group of compound **2**, allowed for the rationalization of glycosylating the Green Research Group's **L2** molecule using the pathway shown in Scheme 5, as a means to ultimately isolating compound **8**. While compound **8** provided its own unique properties and synthetic challenges, path 1a (Scheme 8) gave insight into solvents, catalysts, methods for obtaining solid product, and characterization. This information is vital to preventing unnecessary loss of the expensive and difficult to synthesize compound **7** through experimental reactions.

Path 1b:

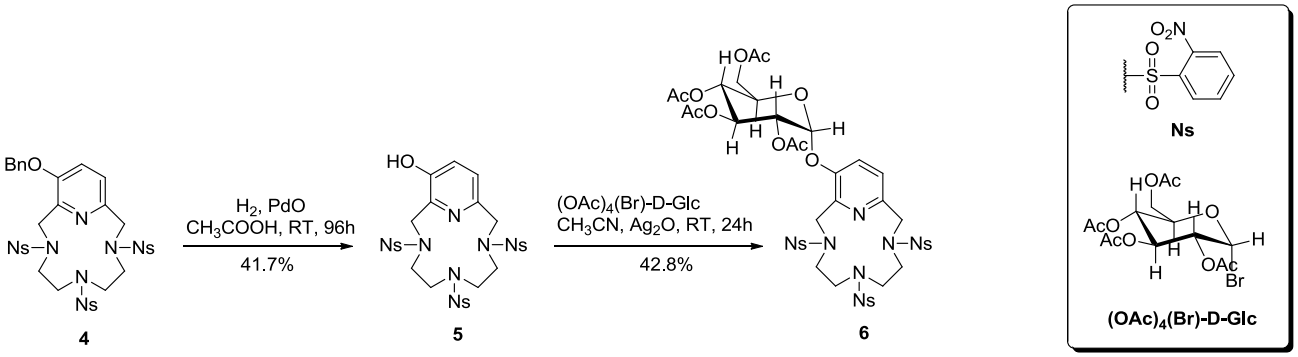

Scheme 9. Synthetic pathway used to produce **6**.

As the **L2** and **L3** ligands have unique properties, a separate control reaction was necessary to assess the reactivity and solubility of **L3** in glycosylation. These unique properties proved to be sufficiently varied from the reaction described above, to warrant altered reaction conditions in the first step of path 1b (Scheme 2). Compound **4** was readily soluble in acetic acid, a solvent that would not allow for benzyl deprotection of compound **2** in path 1a (Scheme 1). Additionally, the product isolated from this step was not as pure as the product in path 1a. A

thin-layer chromatography (5% methanol in dichloromethane) showed that this product was likely a mixture of 3 species. To separate these compounds and to purify compound **5**, column chromatography (5% methanol in dichloromethane, silica) was performed. Three unique fractions were isolated and mass spectrometry data was acquired for each fraction. Fraction 1 showed m/z: $[M + H]^+$ Calcd for $C_{29}H_{28}N_7O_{13}S_3$ 778.0907; Found 778.2297. The solvent from the first fraction was removed under reduced pressure, resulting in a pure solid (41.7% yield) from which the NMR data was taken. The ^1H and ^{13}C NMR spectra confirmed that the benzyl moiety of compound **4** was removed through the hydrogenation process to produce compound **5.**

As shown in Scheme 9, the glycosylation methods used to produce compound **6** from compound **5** proceeded through identical reaction conditions described for the isolation of compound **3**. Compound **5** provided a greater solubility in acetonitrile compared to compound **2**, but the product yields from these reactions were, surprisingly, still quite similar (Compound **3**, 38.0%; Compound **6**, 42.8%). As described above for compound **3,** a similar difficulty was encountered in isolating compound **6** as a solid, and just as in path 1a, the best method seemed to be extensive drying on a Schlenk line and lyophilizer. Compound **6** was characterized using ^1H NMR and ^{13}C NMR to verify the connectivity shown in Scheme 9.

Path 2:

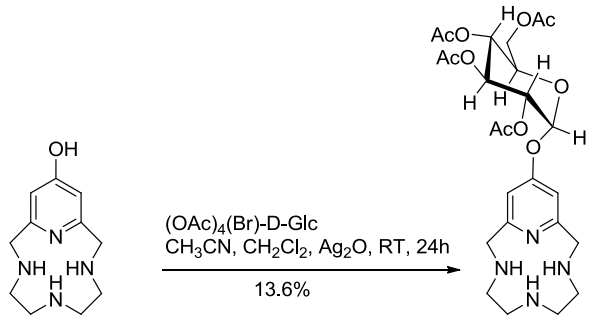

7 **8**

Scheme 5. Synthetic pathway used to produce **8**.

With the control experiments complete, glycosylation was carried out on compound **7** to produce compound **8** using the reaction conditions described above for the synthesis of compounds **3** and **6**. However, the precursor compound **7** was completely insoluble in acetonitrile solution, therefore a mixture of acetonitrile and dichloromethane was employed for the reaction shown in scheme 5. This solvent system still provided incomplete solubility but improved from acetonitrile alone. The remainder of the reaction conditions and the work-up procedures remained nearly identical to the set of control reactions.

Mass spectrometry confirmed the presence of the addition of the protected glucose molecule to compound **7**, but there was initially concern about addition to the amine nitrogen atoms instead of the phenol –OH moiety. The NMR data could not be used to determine connectivity. Specifically, the alpha proton of the glucose (5.395 ppm) was lower than predicted for an O-linked glucose. Therefore, N-atom addition could not be ruled out. To differentiate between O-atom or N-atom addition, two control reactions were performed.

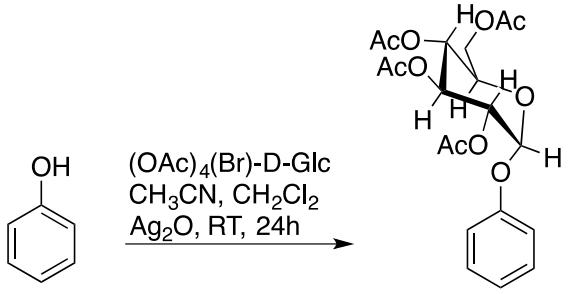

Scheme 10. Control reaction of O-linked glycosylation.

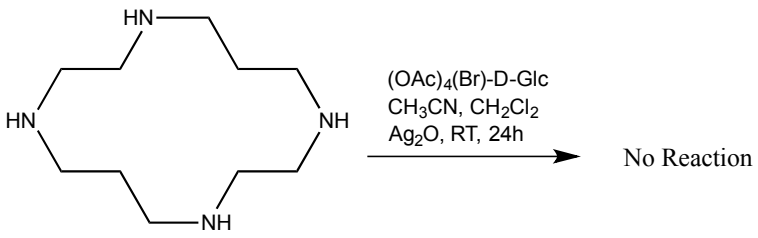

Scheme 11. Control reaction of N-linked glycosylation.

The control reactions shown in schemes 9 and 10 were run under identical conditions to those described for the synthesis of compound 8. Following workup and product isolation, ^{1}H and ^{13}C NMR were obtained in DMSO-d_6 to locate the α-proton of the glucose. The phenol control reaction (Scheme 10) provided a ^{1}H NMR spectrum with a resonance at 5.394 ppm consistent with the α-proton observed in Compound **8** (5.395 ppm). Additionally, this spectrum, as a whole, had many features congruent with the ^{1}H NMR of Compound **8**. Even more interesting, the ^{1}H NMR of the solid isolated from the cyclam control reaction (Scheme 11) was nearly identical to the ^{1}H NMR of the $(OAc)_4$(Br)-D-Glc starting material, suggesting that no reaction had occurred. Additionally, a mass spectrometry of this cyclam control 'product' showed cyclam only (m/z: $[M + H]^+$ Calcd for $C_{10}H_{24}N_4$ 201.34; Found 201.2217). Furthermore, a colleague in my lab, Sean Rodich was working with a similar glycosylation reaction in the addition of galactose to a phenol (Scheme 6).[19] In his characterization, he measured the α-proton (d) at 5.669 ppm as shown in figure 18. This is also quite lower than predicted, but it agrees with the control reactions and path 2a. With the cyclam control reaction suggesting that the amine nitrogen atoms of compound **7** were not reactive to act as glycosyl acceptors and the nearly identical alpha proton resonance of the phenol control, it was concluded that the glucose was successfully added to the phenol of compound **7,** thereby validating the direct methodology for glycosylation of ligands **L2** and **L3** through the use of silver catalysts.

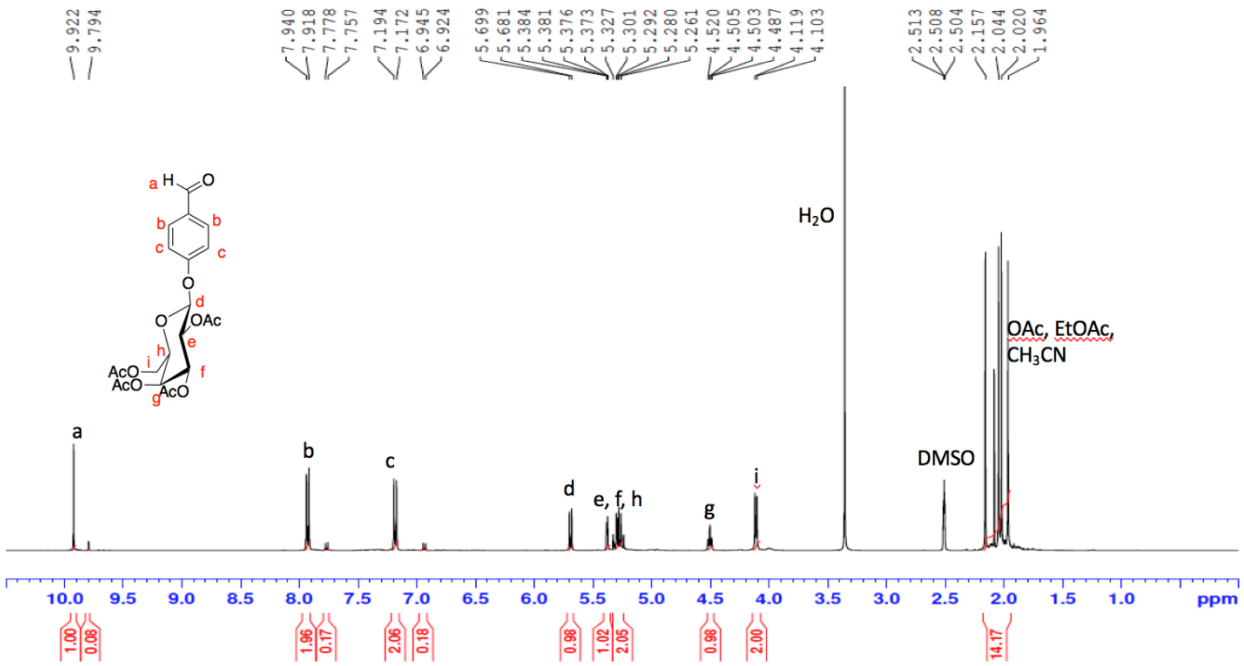

Figure 18. [1]H NMR of Sean Rodich's galactose product in DMSO with labeled molecular diagram.[19]

Conclusion

This study reports the first glycosylated N-heterocyclic amine in literature as well as the first derivatization of **L2** and **L3**. These molecules have many future medicinal applications, and this report can open up a whole new realm of studies on these versatile molecules.

The next steps for this project begin with the optimization of the glycosylation reactions. A more efficient synthesis will be necessary to make enough glycosylated ligand to begin biological studies. Optimization will first require finding a solvent which **L2** and **L3** are more soluble in. This will require the exploration of unconventional glycosylation solvents such as dioxane or DMF.[21] Additionally, these reactions might be optimized by the addition of an organic base, such as triethylamine, to promote better nucleophilicity of the pyridol ring. Finally, it should be noted that the acetyl protecting groups will be removed prior to biological studies via acid work-up.

Biological assays will then be conducted to assess and compare the properties of the glycosylated ligands to **L2** and **L3**. Cytotoxicity, antioxidant activity, and blood brain barrier permeability studies are currently planned for these new ligands.

REFERENCES

(1) Alzheimer's, A. *Alzheimers Dement* **2015**, *11*, 332.

(2) Kenche, V. B.; Barnham, K. J. *Br J Pharmacol* **2011**, *163*, 211.

(3) Lincoln, K. M.; Gonzalez, P.; Richardson, T. E.; Julovich, D. A.; Saunders, R.; Simpkins, J. W.; Green, K. N. *Chemical Communications* **2013**, *49*, 2712.

(4) Lincoln, K. M.; Richardson, T. E.; Rutter, L.; Gonzalez, P.; Simpkins, J. W.; Green, K. N. *ACS Chem Neurosci* **2012**, *3*, 919.

(5) Egleton, R. D.; Mitchell, S. A.; Huber, J. D.; Palian, M. M.; Polt, R.; Davis, T. P. *J Pharmacol Exp Ther* **2001**, *299*, 967.

(6) Lincoln, K. M.; Gonzalez, P.; Richardson, T. E.; Julovich, D. A.; Saunders, R.; Simpkins, J. W.; Green, K. N. *Chem. Commun* **2013**, *49*, 2712.

(7) Lincoln, K. M.; Offutt, M. E.; Hayden, T. D.; Saunders, R. E.; Green, K. N. *Inorg Chem* **2014**, *53*, 1406.

(8) Duelli, R.; Kuschinsky, W. *News Physiol. Sci.* **2001**, *16*, 71.

(9) Sajja, R. K.; Green, K. N.; Cucullo, L. *PLOS* **2015**, *10*, e0122358.

(10) Green, D. E.; Bowen, M. L.; Scott, L. E.; Storr, T.; Merkel, M.; Bohmerle, K.; Thompson, K. H.; Patrick, B. O.; Schugar, H. J.; Orvig, C. *Dalton T* **2010**, *39*, 1604.

(11) Schugar, H.; Green, D. E.; Bowen, M. L.; Scott, L. E.; Storr, T.; Bohmerle, K.; Thomas, F.; Allen, D. D.; Lockman, P. R.; Merkel, M.; Thompson, K. H.; Orvig, C. *Angew Chem Int Edit* **2007**, *46*, 1716.

(12) Storr, T.; Merkel, M.; Song-Zhao, G. X.; Scott, L. E.; Green, D. E.; Bowen, M. L.; Thompson, K. H.; Patrick, B. O.; Schugar, H. J.; Orvig, C. *J Am Chem Soc* **2007**, *129*, 7453.

(13) Rovner, S. E. In *C&E News* American Chemical Society: C&E News, 2009, p 42.

(14) Burns, J. M.; Donnelly, J. E.; Anderson, H. S.; Mayo, M. S.; Spencer-Gardner, L.; Thomas, G.; Cronk, B. B.; Haddad, Z.; Klima, D.; Hansen, D.; Brooks, W. M. *Neurology* **2007**, *69*, 1094.

(15) Reger, M. A.; Watson, G. S.; Green, P. S.; Wilkinson, C. W.; Baker, L. D.; Cholerton, B.; Fishel, M. A.; Plymate, S. R.; Breitner, J. C. S.; DeGroodt, W.; Mehta, P.; Craft, S. *Neurology* **2008**, *70*, 440.

(16) Lincoln, K. M.; Richardson, T. E.; Rutter, L.; Gonzalez, P.; Simpkins, J. W.; Green, K. N. *Acs Chem Neurosci* **2012**, *3*, 919.

(17) Lipinski's rules : (low molecular weight (MW ≤ 450), relatively lipophilic (c log P, calculated logarithm of the octanol/water partition coefficient, ≤5), hydrogen-bond donor atoms (HBD ≤ 5), hydrogen-bond acceptor atoms (HBA ≤ 10), small polar surface area (PSA ≤ 90 °A2). .

(18) Lipinski, C. A.; Lombardo, F.; Dominy, B. W.; Feeney, P. J. *Advanced Drug Delivery Reviews* **2001**, *46*, 3.

(19) Chauvin, T.; Durand, P.; Bernier, M.; Meudal, H.; Doan, B. T.; Noury, F.; Badet, B.; Beloeil, J. C.; Toth, E. *Angew Chem Int Ed Engl* **2008**, *47*, 4370.

(20) Jensen, K. J.; Meldal, M.; Bock, K. *J Chem Soc Perk T 1* **1993**, 2119.

(21) Jensen, K. J. *J Chem Soc Perk T 1* **2002**, 2219.